Article

Analyzing the Bianchi Type-I Universe with a Special Form of Deceleration Parameter in $f(T)$ Gravity

Syed M. S. Iqbal* & G. U. Khapekar

Dept. of Math., Jagadamba Mahavidyalaya, Achalpur City, Achalpur Maharashtra, India

Abstract

This paper investigates the homogeneous and anisotropic Bianchi type-I spacetime within the framework of $f(T)$ gravity theory, utilizing a quadratic equation of state and a specific deceleration parameter. In this paper, we employ Bayesian statistical methods, utilizing the Markov Chain Monte Carlo (MCMC) technique, to estimate model parameters such as ξ and the Hubble constant H_0 using the Cosmic Chronometers (CC) dataset. Our analysis yields $\xi = 1.49^{+0.10}_{-0.10}$ and $H_0 = 65.04^{+2.47}_{-2.39}$. we conduct a thorough and detailed analysis of the model's behavior via energy density (ρ), pressure (p), anisotropic parameter (A_m), torsion scalar (T), deceleration parameter (q) as a function of redshift z. The physical acceptance and stability of the model are examined by analyzing energy conditions and the squared sound speed (ϑ_s^2). Furthermore, all cosmological parameters are graphically illustrated to enhance our understanding of the universe's expansion and evolutionary history. In addition, the diagnostic parameters are analyzed to assess the deviation of the obtained model from the Lambda Cold Dark Matter (ΛCDM) model and to classify dark energy models during the expansion. Finally, our obtained model represents the transition of the universe from an early deceleration phase to the recent accelerated expansion phase. The universe exhibits anisotropic characteristics at present but is expected to become isotropic in the future. Ultimately, the behavior of our model aligns with that of a quintessence dark energy model.

Keywords: Bianchi Type-I universe, quadratic equation of state, cosmic chronometers, special form of deceleration parameter, $f(T)$-gravity.

1. Introduction

Since the inception of the Big Bang, the universe has been expanding persistently, with its rate of expansion accelerating over time, a phenomenon that continues unabated to the present day. This phenomenon has been validated through several astrophysical and cosmological observations, including Type Ia supernovae (SNe Ia) [1, 2], the cosmic microwave background radiation [3, 4, 5], and the study of large-scale structures (LLS) [6]. However, the exact cause of this accelerated

*Correspondence: Syed M. S. Iqbal, Dept. of Math., Jagadamba Mahavidyalaya, Achalpur City, Achalpur Maharashtra, India.
E-mail: muddumsc@gmail.com

expanding universe phenomenon remains a subject of investigation. Cosmologists and astronomers commonly suggest the existence of dark energy (DE) in the universe to address this phenomenon.

Dark energy is believed to be an unknown form of energy with negative pressure that, along with cold dark matter (CDM), significantly impacts the universe. The interaction of dark energy and cold dark matter is considered the primary driver of the universe's recent accelerated expansion. The ΛCDM (cold dark matter) model effectively explains various physical phenomena such as the formation and evolution of large-scale structures in the universe, early universe dynamics, and the distribution of matter and energy.

Despite its successes, the model struggles to account for the remarkably low observed value of dark energy density, particularly when compared with predictions from quantum field theories. This challenge is referred to as the cosmological constant problem [7, 8]. Recent research has also questioned the ΛCDM model's predictions regarding the age of the universe [9], prompting renewed interest in exploring alternative theories to explain the universe's current accelerated expansion.

By modifying the geometric component of Einstein's Hilbert action, a multitude of innovative theories of gravity have emerged, aiming to unravel the mystery of cosmic acceleration. These include the $f(R)$ theory of gravity [10], which centers on the Ricci scalar (R); the $f(G)$ theory of gravity [11], focusing on the Gauss-Bonnet invariant (G) ; the $f(R,T)$ theory of gravity [12], incorporating both the Ricci scalar (R) and the trace of the energy-momentum tensor (T); and the $f(T)$ theory of gravity [13], which revolves around the torsion scalar (T). These diverse approaches not only challenge traditional paradigms but also strive to provide compelling explanations for the ongoing expansion of the universe, marking a bold frontier in theoretical cosmology.

In the domain of modified theories of gravity, the $f(T)$ theory of gravity stands out due to its unique attributes. Significantly, it successfully accounts for the universe's current accelerated expansion without requiring a dark energy component. Furthermore, in contrast to the $f(R)$ theory of gravity, which involves complex fourth-order field equations, the $f(T)$ theory simplifies the process with second-order field equations. This simplification is achieved through the use of the Weitzenböck connection, which avoids the curvature associated with the Levi-Civita connection used in general relativity (GR) and the $f(R)$ theory, focusing instead on torsion. The torsion in this theory arises solely from the first derivatives of the tetrad, with no second derivatives involved in the formation of the torsion tensor, highlighting the distinctiveness of this approach.

The $f(T)$ theory of gravity, introduced by Bengochea and Ferraro [13-15], is an extension of teleparallel gravity [16,17]. Teleparallel gravity was initially developed by Einstein in an attempt to unify gravity and electromagnetism [18,19]. Myrzakulov [20] has explored the concept of the accelerating universe using the framework of $f(T)$ theory of gravity. Mandal et al. [21] have investigated the accelerating universe in hybrid and logarithmic teleparallel gravity. Their study aims to leverage the attractive features of $f(T)$ gravity to propose various cosmological scenarios. Shekh and Chirde [22] explored certain characteristics of an accelerating anisotropic Bianchi type-I cosmological model, considering the presence of two non-interacting fluids: a conventional cosmic string and a dark energy fluid.

Pawar and Dagwal [23] have introduced tilted cosmological models within the framework of $f(T)$ gravity theory. Koussour and Bennai [24] conducted an analysis of an anisotropic Bianchi type-I cosmological model within the framework of teleparallel gravity, considering the presence of a perfect fluid. Pawar et al. [25] conducted an investigation into the dynamics of homogeneous and anisotropic LRS Bianchi type-I spacetime using $f(T)$ gravity, taking into account the influence of a perfect fluid with heat flow. Dagwal [26] investigated the tilted model utilizing forms of dark energy, including components of quintessence and cosmological constant, within the framework of $f(T)$ theory of gravity.

Duchaniya et al. [27] conducted a dynamical system analysis of the $f(T)$ theory of gravity, considering three distinct models: the logarithmic model, the power law model, and a combination of the first two models. Briff et al. [28] have studied the flat Friedmann–Lemaître–Robertson–Walker (FLRW) universe using redshift space distortion within the framework of $f(T)$ cosmology, which sheds light on cosmic evolution. Dimakis et al. [29] have studied the quantum cosmology using the FLRW universe within the framework of teleparallel $f(T)$ gravity. These investigations have produced significant findings and provided valuable insights into the behavior of gravitational theories beyond general relativity.

In the fields of relativity and cosmology, the equation of state is crucial as it establishes the relationship between matter, temperature, pressure, and energy density in any region of space. The quadratic equation of state is especially significant in Brane world models and the investigation of dark energy and general relativistic dynamics in various models [30, 31]. Moreover, this equation of state dictates the universe's evolution from the Planck epoch to the de-Sitter epoch, underscoring its growing importance. the quadratic equation of state has the potential to characterize dark energy or even a unified form of dark energy [32]. Thus, examining the quadratic equation of state is essential. The general form of the quadratic equation of state can be expressed as:

$$p = p_0 + \omega\rho + \alpha\rho^2 \tag{1}$$

Here p and ρ are the pressure and energy density respectively. p_0 , ω , α are the parameters. In this research, we examine the quadratic equation of state, specifically considering the conditions $p_0 = 0$ and $\omega = -1$ [33]. Under these assumptions, the equation simplifies to:

$$p = -\rho + \alpha\rho^2 \tag{2}$$

where $\alpha \neq 0$ is a constant.

Singh and Bishi [34] explored the Bianchi type-I cosmological model within the framework of $f(R,T)$ modified gravity using quadratic equation of state. Chavanis [35] investigated a cosmological model utilizing a quadratic equation of state to describe the universe's evolution, capturing early inflation, intermediate decelerating expansion, and late accelerating expansion. Bhoyar and Shekh [36] have delved into the properties of the Bianchi type-I space-time under a quadratic equation of state within the $f(R)$ gravity framework. Their investigation utilized the volumetric power law and the exponential law of expansion to thoroughly examine the dynamic behavior and evolution of this cosmological model.

Thakare and Mapari [37] have investigated the five-dimensional plane symmetric cosmological model incorporating a quadratic equation of state within the framework of $f(R,T)$ gravity theory. Their study applied both the volumetric power law and the exponential law of expansion to derive precise solutions, providing deeper insights into the model's behavior and characteristics. Mahanta and Deka [38] have studied the Bianchi type V universe with a time-varying cosmological constant and a quadratic equation of state within the framework of $f(R,T)$ gravity theory.

Inspired by the research mentioned earlier, we are analyzing the Bianchi type I universe with quadratic equation of state and a special form of deceleration parameter in $f(T)$ gravity using Cosmic Chronometers. The structure of this article is organized as follows: In Section 2, we cover the basic mathematical framework of $f(T)$ theory of gravity. We also derived the field equations for Bianchi type-I and present their solution. In Section 3, we compare our cosmological model with Cosmic Chronometers (CC) dataset to determine model parameters such as ξ and H_0 .

To achieve this, we use Bayesian statistical methods and the Markov Chain Monte Carlo (MCMC) technique. In Section 4, the dynamical nature of the universe has been studied using cosmological parameters such as energy density, pressure and anisotropic parameter etc. Furthermore, we examined the stability parameter, energy conditions, and diagnostic parameters such as Statefinder diagnostic parameter and O_m diagnostic parameter in the same section. Finally, Section 5 provides summary and concluding remarks of this article.

2. Foundations of $F(T)$ Theory of Gravity and Bianchi Type-I Cosmology

Firstly, we will explore some mathematical framework and geometrical foundations associated with $f(T)$ theory of gravity. Thus, we will begin by discussing how the action of $f(T)$ theory of gravity is defined [39,40]:

$$S = \frac{1}{16\pi G}\int e\, f(T)\; d^4x + \int e\, \mathcal{L}_m\, d^4x \tag{3}$$

where $f(T)$ is the arbitrary function of Torsion scalar T, the expression $\mathcal{L}_m$ stand for the matter Lagrangian density. Here $e = det\left(e_\mu^i\right) = \sqrt{-\mathrm{g}}$ with e_μ^i serving as the tetrad (vierbein) field employed as a dynamic element in teleparallel gravity. Its inverse, denoted by e_i^μ, satisfies the relations $e_\mu^i . e_j^\mu = \delta_j^i$ and $e_\mu^i . e_i^\nu = \delta_\mu^\nu$. Furthermore, G denotes the Newtonian gravitational constant. The torsion scalar (T) is defined as

$$T = T^\alpha{}_{\mu\nu}\, S_\alpha{}^{\mu\nu} \tag{4}$$

The torsion tensor $T^\alpha{}_{\mu\nu}$ and sometimes referred to as the superpotential tensor $S_\alpha{}^{\mu\nu}$ are defined as

$$T^\alpha{}_{\mu\nu} = \Gamma^\alpha{}_{\nu\mu} - \Gamma^\alpha{}_{\mu\nu} = e_i^\alpha\left(\partial_\mu e_\nu^i - \partial_\nu e_\mu^i\right) \tag{5}$$

$$S_\alpha{}^{\mu\nu} = \frac{1}{2}\left(K^{\mu\nu}{}_\alpha + \delta_\alpha^\mu\, T^{\beta\nu}{}_\beta - \delta_\alpha^\nu\, T^{\beta\mu}{}_\beta\right) \tag{6}$$

Where the Weitzenbock connection $\Gamma^\alpha{}_{\mu\nu}$ and contorsion tensor $K^{\mu\nu}{}_\alpha$ are defined as follows:

$$\Gamma^\alpha{}_{\mu\nu} = e_i^\alpha\, \partial_\nu\, e_\mu^i = -\, e_\mu^i\, \partial_\nu\, e_i^\alpha \tag{7}$$

$$K^{\mu\nu}{}_\alpha = -\frac{1}{2}\left(T^{\mu\nu}{}_\alpha - T^{\nu\mu}{}_\alpha - T_\alpha{}^{\mu\nu}\right) \tag{8}$$

Note that the contorsion tensor is the difference between the weitzenbock connection and the Levi-Civita connection. By taking the variation of the action (3) with respect to the tetrads, one can derive the field equations in modified teleparallel gravity with $f(T)$ as

$$S_\mu{}^{\nu\rho}\left(\partial_\rho T\right) f_{TT} + \left[e^{-1} e_\mu^i\, \partial_\rho\left(e\, e_i^\alpha\, S_\alpha{}^{\nu\rho}\right) + T^\alpha{}_{\lambda\mu} S_\alpha{}^{\nu\lambda}\right] f_T + \frac{1}{4}\delta_\mu^\nu\, f = 4\pi G T_\mu^\nu \tag{9}$$

where $f_T = \frac{df}{dT}$, $f_{TT} = \frac{d^2 f}{dT^2}$ and T_μ^ν is the energy-momentum tensor of the particular matter. In this study, our focus is on a perfect fluid characterized by

$$T_{\mu\nu} = (p + \rho) u_\mu u_\nu - p g_{\mu\nu} \tag{10}$$

where ρ and p are energy density and pressure of the fluid respectively and $u^i = (0,0,0,1)$ be the four-velocity vector of the fluid which satisfying the condition $u^\mu u_\mu = 1$. Following the inflationary epoch, the Universe tends towards homogeneity and isotropy [41], as indicated by many studies.

However, defects in the cosmic microwave background (CMB) from quantum fluctuations during inflation suggest an initial anisotropic phase transitioning into isotropy. Recent Planck data [42] has highlighted Bianchi cosmological models, which specifically describe an anisotropic Universe, garnering considerable attention. The literature covers a range of anisotropic and inhomogeneous Bianchi spacetimes, with Bianchi type-I spacetime particularly notable for its mathematical simplicity. It represents an anisotropic yet homogeneous Universe, much like an extension of the FLRW model, where each spatial direction features distinct scale factors.

Numerous studies have explored different Bianchi type-I cosmological models across various research contexts. Saaidi et al. [43] explore the dynamic evolution of an $f(R)$ gravity model within a viscous and anisotropic background, specifically characterized by Bianchi type-I space-time. Hossienkhani et al. [44] investigated the spatially homogeneous and anisotropic Bianchi type-I Universe using models of dark energy (DE) that involve interacting holographic and new agegraphic scalar fields.

Recently, Koussour and Bennai [45] have studied the spatially homogeneous anisotropic Bianchi type-I Universe with cubically varying deceleration parameter in $f(R,T)$ gravity. Bhoyar et al. [46] explored cosmological models of anisotropic spatially homogeneous Bianchi type-I in the context of Lyra's manifold, utilizing the normal gauge. Many authors, such as Banerjee et .al [47, 48], Krori et al [49], Xulu [50], Salti et. al [51], Vargas et. al [52] have studies the Bianchi type-I spacetime with distinct exponential form of scale factors in each spatial direction. Motivated by these studies, we selected the homogeneous and anisotropic

Bianchi type-I spacetime, defined by:

$$ds^2 = dt^2 - e^{2l}dx^2 - e^{2m}dy^2 - e^{2n}dz^2 \tag{11}$$

where the metric potentials e^l, e^n, e^m are the functions of cosmic time t only and x, y, z are the usual cartesian co-ordinates. The set of all diagonal tetrads corresponding to the spacetime given in equation (11) is

$$e^i_\mu = diag\,(1, e^l, e^m, e^n) \tag{12}$$

The corresponding spatial volume, Hubble parameter and Anisotropic parameters are defined as

$$V = a^3 = exp(l + m + n) \tag{13}$$

$$H = \frac{1}{3}\frac{\dot{V}}{V} = \frac{1}{3}\left(\dot{l} + \dot{m} + \dot{n}\right) \tag{14}$$

$$A_m = -1 + \frac{3\left(\dot{l}^2 + \dot{m}^2 + \dot{n}^2\right)}{\left(\dot{l} + \dot{m} + \dot{n}\right)^2} \tag{15}$$

The torsion scalar T for the Bianchi type I spacetime given in equation (11) as

$$T = -2\left[\dot{l}\dot{m} + \dot{l}\dot{n} + \dot{m}\dot{n}\right] \tag{16}$$

By utilizing equation (11) alongside the energy-momentum tensor provided in equation (10), the field equations (9) for Bianchi type-I spacetime can be derived as follows:

$$f + 4f_T\left(\dot{l}\dot{m} + \dot{l}\dot{n} + \dot{m}\dot{n}\right) = \kappa^2\rho \tag{17}$$

$$f + 2f_T\left[(\ddot{m} + \ddot{n}) + \left(\dot{m} + \dot{n} + \dot{l}\right)(\dot{m} + \dot{n})\right] + 2(\dot{m} + \dot{n})\dot{T}f_{TT} = -\kappa^2 p \tag{18}$$

$$f + 2f_T\left[\left(\ddot{l} + \ddot{n}\right) + \left(\dot{m} + \dot{n} + \dot{l}\right)\left(\dot{l} + \dot{n}\right)\right] + 2\left(\dot{l} + \dot{n}\right)\dot{T}f_{TT} = -\kappa^2 p \tag{19}$$

$$f + 2f_T\left[\left(\ddot{l} + \ddot{m}\right) + \left(\dot{m} + \dot{n} + \dot{l}\right)\left(\dot{l} + \dot{m}\right)\right] + 2\left(\dot{l} + \dot{m}\right)\dot{T}f_{TT} = -\kappa^2 p \tag{20}$$

where the dot $(\cdot)$ denotes the derivative with respect to cosmic time t. In this paper, we assume $\kappa^2 = 16\pi G \cong 1$ for calculation simplicity. The set of equations (17)-(20) constitutes a system of four differential equations, which involve six unknowns such as $l, m, n, f(T), \rho(t)$ and $p(t)$. To explicitly solve these field equations, two additional constraints are required. Firstly, we employ the linear form of $f(T)$ gravity, specifically

$$f(T) = \xi_1 T + \xi_2 \tag{21}$$

After solving equations (18) to (20) through subtraction and utilizing equations (13) and (21), we found as

$$l - m = k_1 \int \frac{1}{V}\, dt + \chi_1 \tag{22}$$

$$l - n = k_2 \int \frac{1}{V}\, dt + \chi_2 \tag{23}$$

$$m - n = k_3 \int \frac{1}{V}\, dt + \chi_3 \tag{24}$$

where $k_i\ (i = 1,2,3)$ and $\chi_i\ (i = 1,2,3)$ are constants of integrations which satisfied the relation $k_2 = k_1 + k_3$ and $\chi_2 = \chi_1 + \chi_3$.

Finally, we can represent l, m and n explicitly as

$$l = \frac{1}{3}\log V + \zeta_1 \int \frac{1}{V}\, dt + \eta_1 \tag{25}$$

$$m = \frac{1}{3}\log V + \zeta_2 \int \frac{1}{V}\, dt + \eta_2 \tag{26}$$

$$n = \frac{1}{3}\log V + \zeta_3 \int \frac{1}{V}\, dt + \eta_3 \tag{27}$$

where $\zeta_i\ (i = 1,2,3)$ and $\eta_i\ (i = 1,2,3)$ are the constants which satisfies the relation $\sum_{i=1}^{3}\zeta_i = 0$ and $\sum_{i=1}^{3}\eta_i = 0$.

For obtaining the exact solutions to the field equations, we are utilizing the special form deceleration parameter (DP) as the second constraint. The Special form of deceleration parameter [53] defined as

$$q = -\frac{\ddot{a}a}{\dot{a}^2} = -1 + \frac{\xi}{1+a^{\xi}} \tag{28}$$

In which, ξ represents a positive constant, and a denotes the scale factor of the Universe. The deceleration parameter (DP) serves as a crucial metric for understanding the evolution of the Universe over time. Initially, a positive value of the DP $(q > 0)$ denotes a phase dominated by cosmic deceleration. However, recent observational data from sources such as Type Ia Supernovae (SNe Ia) suggest a transition from this decelerating phase to an accelerating one, denoted by a negative value of the DP $(q < 0)$. This shift signifies a remarkable evolution from deceleration to acceleration in the Universe's expansion.

Solving Equation (28), we found the scale factor (a) of the universe as

$$a(t) = \left(e^{\xi kt} - 1\right)^{\frac{1}{\xi}} \tag{29}$$

where k is the constant of integration.

The Hubble parameter, represents the rate of expansion of the universe and expressed as $H = \frac{\dot{a}}{a}$, where $\dot{a}$ represents the time derivative of the scale factor of the universe a, obtained as

$$H(t) = \frac{ke^{\xi kt}}{\left(e^{\xi kt}-1\right)} \tag{30}$$

From the definition of spatial volume in terms of the average scale factor, i.e., $V = a^3$, and utilizing Equation (29) in equations (25) to (27), we obtain the corresponding metric potentials as.

$$e^{l} = C_1\left(e^{\xi kt} - 1\right)^{\frac{1}{\xi}} exp\left(\zeta_1 \int \left(e^{\xi kt} - 1\right)^{-\frac{3}{\xi}} dt\right) \tag{31}$$

$$e^{m} = C_2\left(e^{\xi kt} - 1\right)^{\frac{1}{\xi}} exp\left(\zeta_2 \int \left(e^{\xi kt} - 1\right)^{-\frac{3}{\xi}} dt\right) \tag{32}$$

$$e^{n} = C_3\left(e^{\xi kt} - 1\right)^{\frac{1}{\xi}} exp\left(\zeta_3 \int \left(e^{\xi kt} - 1\right)^{-\frac{3}{\xi}} dt\right) \tag{33}$$

In which, $C_i = e^{\eta_i}, (i = 1,2,3)$, satisfy the condition $\prod_{i=1}^{3} C_i = 1$. Additionally, the solution to the integral $\int \left(e^{\xi kt} - 1\right)^{-\frac{3}{\xi}} dt$ is a hypergeometric function. Due to the complexity of working with hypergeometric functions, we will retain the integral in its current form. One more thing to note here is that in the subsequent calculations, this integration cancels out with a derivative.
In cosmology, the relationship between the scale factor of the universe and cosmological redshift (z) is expressed as $a = a_0(1 + z)^{-1}$, where a_0 represent the current value of scale factor of the universe, as a standard convention or for the calculation simplicity, we set $a_0 = 1$. Applying this relation to equation (29), we get the cosmic time- redshift relation as

$$t(z) = \frac{1}{\xi k} log\left(\frac{(z+1)^{\xi}+1}{(z+1)^{\xi}}\right) \tag{34}$$

Utilizing equation (29) in equation (30), we obtain the expression for the Hubble parameter with respect to redshift z as

$$H(z) = \frac{H_0\left((z+1)^{\xi}+1\right)}{2} \tag{35}$$

3. Analysis With Observational Dataset

In this section, we perform a comprehensive comparison between our obtained cosmological model and various available cosmological data to understand its fundamental characteristics. We focus on dataset from Cosmic Chronometers (CC) to determine the optimal values of key model parameters, such as ξ. This investigation also includes the present-day Hubble constant, H_0 , which significantly influences our results. To achieve the best fit values for our model, we employ a robust Bayesian statistical methodology, utilizing likelihood functions and the Markov Chain Monte Carlo (MCMC) technique [54]. Specifically, we use the Python `emcee` package for the MCMC analysis, running 200 walkers for 1000 steps to obtain our results. This approach helps ensure the reliability and precision of our parameter estimations.

The ΛCDM model, widely regarded as the standard model of cosmology, has gained acceptance because it effectively accounts for numerous observed phenomena. These include the Universe's expansion, the cosmic microwave background radiation, and Big Bang nucleosynthesis. The ΛCDM model is defined as

$$H(z) = H_0\sqrt{\Omega_m(1+z)^3 + 1 - \Omega_m} \tag{36}$$

where $\Omega_m = 1 - \Omega_\Lambda$ and Ω_Λ are the matter density parameter and dark energy density parameter, respectively. We will determine the values of Ω_m and H_0 using the same techniques and observational datasets mentioned above. By incorporating these datasets, we aim to provide a holistic understanding of how our model behaves within the framework of $f(T)$ gravity, thereby offering deeper insights into the dynamics of the universe.

The cosmic chronometers (CC) technique, introduced by Jimenez and Loeb [55] in their paper titled “Constraining Cosmological Parameters Based on Relative Galaxy Ages," is a method for estimating the Hubble parameter $H(z)$. This technique involves the spectroscopic determination of the age difference between two passively evolving early-type galaxies. By calculating the differential ages of galaxies as a function of redshift z, the Hubble parameter $H(z)$ can be directly estimated using the following expression:

$$H(z) = -\frac{1}{1+z}\frac{dt}{dz} \tag{37}$$

In this study, we utilize a compilation of **31** measurements of $H(z)$, covering the range $0.07 < z < 1.965$ [56,57,58]. The data is presented in Table 1 (see Appendix). The chi-square [58,59] value for the cosmic chronometers is calculated according to the following definition:

$$\chi^2_{cc}(\xi, H_0) = \sum_{i=1}^{31} \left[\frac{H_{obs}(z_i) - H_{th}(z_i, \xi, H_0)}{\sigma_H(z_i)}\right]^2 \tag{38}$$

where H_{obs} and H_{th} denote the observed and the theoretical value (obtain from the model) of the Hubble parameter, respectively. On the other hand, $\sigma_H(z_i)$ corresponds to the error on the observed values of the Hubble parameter $H(z)$. The analysis results using cosmic chronometer (CC) data with the MCMC technique for both our obtained cosmological model and the ΛCDM model are detailed in Table 2. Figures 1 and 2 display the contour plots, which include the $1-\sigma$ and $2-\sigma$ regions, corresponding to 68% and 95% confidence levels, respectively. Additionally, the Figure 3 shows the error bar plot considering 31 points of cosmic chronometer (CC) datasets together with $H(z)$ versus redshift z for our obtained model compare with standard ΛCDM model.

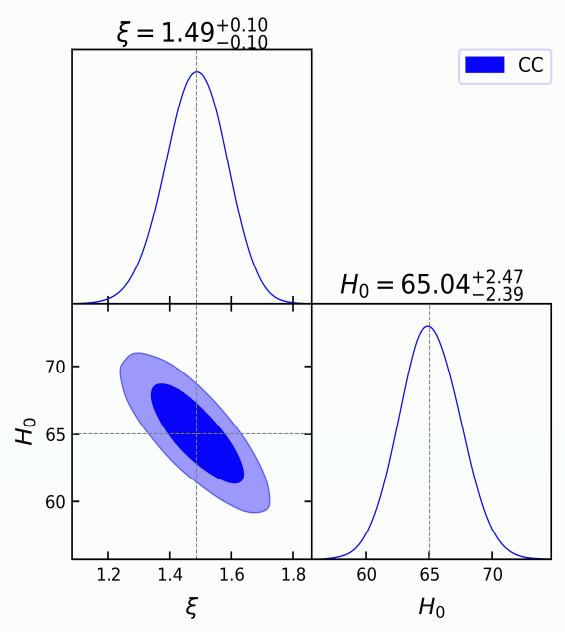

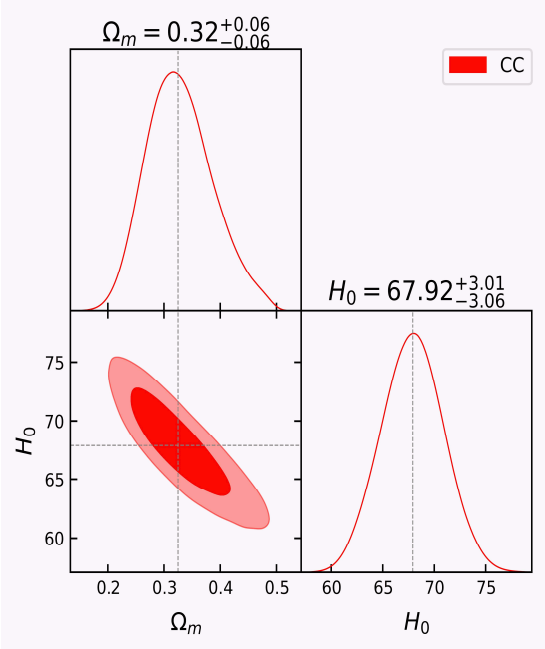

Figure 1: (left) and **Figure 2:** (right) shows the $1-\sigma$ and $2-\sigma$ contour plots for ξ, H_0 and Ω_0, H_0 respectively using CC datasets.

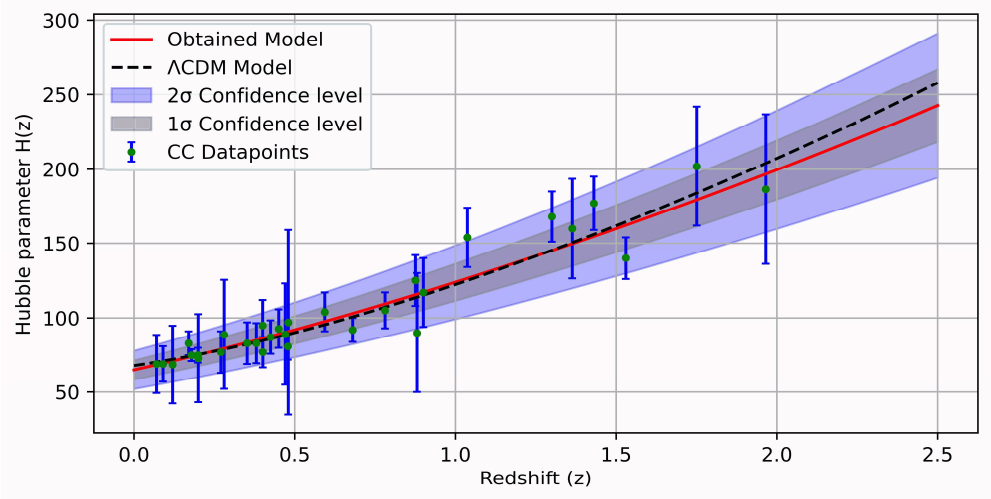

Figure 3: The error bar plot considering 31 points of CC datasets together with $H(z)$ versus redshift z for our obtained model compare with standard ΛCDM model.

Model (CC)	H_0	Ω_m	ξ
ΛCDM	$67.92^{+3.01}_{-3.06}$	$0.32^{+0.06}_{-0.06}$	---
Obtained model	$65.04^{+2.47}_{-2.39}$	---	$1.49^{+0.10}_{-0.10}$

Table 2: MCMC Results for Analysis with CC Datasets

4. Probing Cosmic Evolution and Dynamics

4.1. The energy density (ρ)

Utilizing equations (21), (31) through (33), and (34) in equation (17), the energy density of the universe is obtained as

$$\rho(z) = \xi_1 \left(6k^2\left[(z+1)^{\xi}+1\right]^2 + 2\chi(z+1)^6\right) + \xi_2 \tag{39}$$

Figure 4 depicts the behavior of the universe's energy density in relation to redshift z. The energy density remains consistently positive, increasing with higher redshift z, or conversely, decreasing as cosmic time t progresses. Notably, the energy density is very high in the early universe and gradually diminishes to a small positive value in the future ($i.e. z \to -1 \; or \; t \to \infty$). This trend underscores the continuous expansion of the Universe.

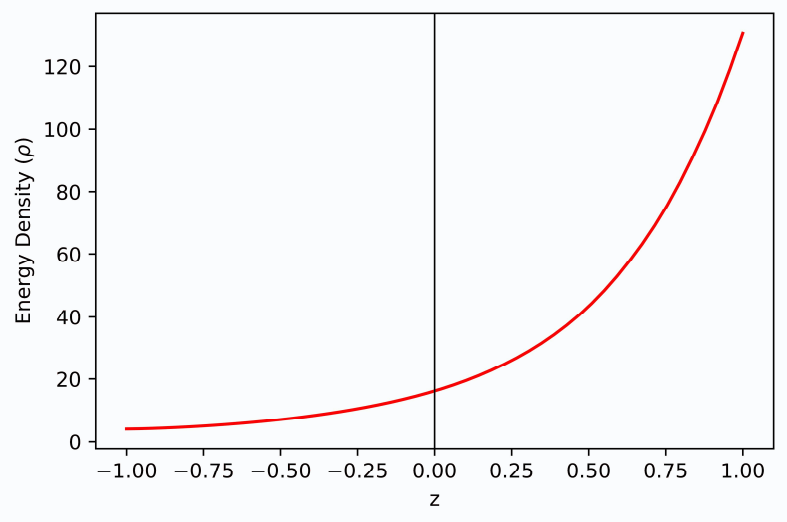

Figure 4: Shows the behavior of ρ versus z.

4.2. The pressure (p)

Utilizing equations (21), (31) through (33), and (34) in equation (18), the pressure of the universe is obtained as

$$p(z) = \left[-1 + \alpha\left\{\xi_1\left(6k^2\left[(z+1)^{\xi}+1\right]^2 + 2\chi(z+1)^6\right) + \xi_2\right\}\right]\left[\xi_1\left(6k^2\left[(z+1)^{\xi}+1\right]^2 + 2\chi(z+1)^6\right) + \xi_2\right] \tag{40}$$

Figure 5 illustrates the pressure behavior of the universe in our model concerning redshift z. The figure clearly demonstrates that the pressure is currently negative and will continue to be negative in the future. This negative pressure indicates the presence of dark energy, which is responsible for the accelerated expansion phase of the universe, as corroborated by astronomical observations.

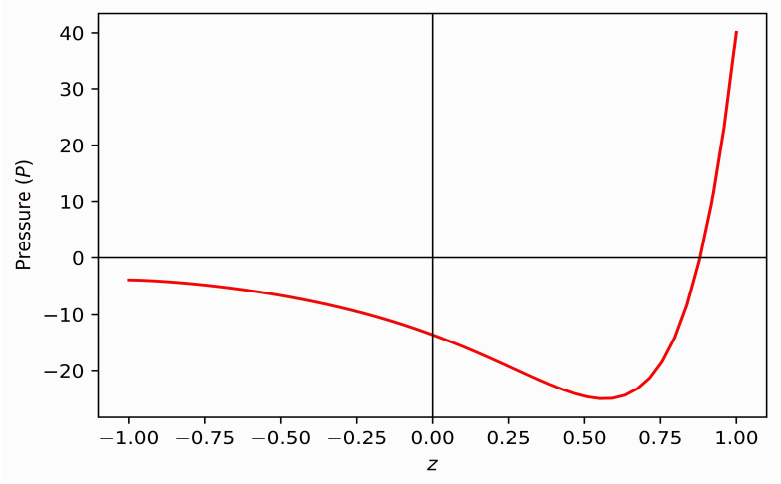

Figure 5: Shows the behavior of p versus z.

4.3. Stability parameter (ϑ_s^2)

The squared sound speed, denoted as ϑ_s^2, serves as a crucial test for analyzing the stability of the universe. It is computed as the ratio of the rate of change of pressure with respect to the rate of change of energy density. When $\vartheta_s^2 > 0$, it indicates a stable universe, if $\vartheta_s^2 < 0$, it signals an unstable universe. Mathematically, it can be expressed [60-62] as:

$$\vartheta_s^2 = \frac{dp}{d\rho} \tag{41}$$

Utilizing equations (39) and (40) in equation (41) yields the speed of sound ϑ_s^2 for our derived model as

$$\vartheta_s^2 = -1 + 2\alpha\left[2\xi_1\left(3k^2\left[(z+1)^{\xi}+1\right]^2 + \chi(z+1)^6\right) + \xi_2\right] \tag{42}$$

Figure 6 illustrates the trend of the squared speed of sound, also known as the stability parameter, concerning redshift for our model. It can be clearly observed that during the early phase of the universe, the squared speed of sound is greater than zero $\vartheta_s^2 > 0$, indicating a stable universe. However, it is currently negative and will remain negative in the future $\vartheta_s^2 < 0$, indicating an unstable universe. Thus, we can conclude from the stability parameter discussion that the universe was stable in its early phase but is now unstable and will continue to be unstable in the future. The redshift $z \simeq 0.57$ marks the point at which the universe in our model transitions from stability to instability.

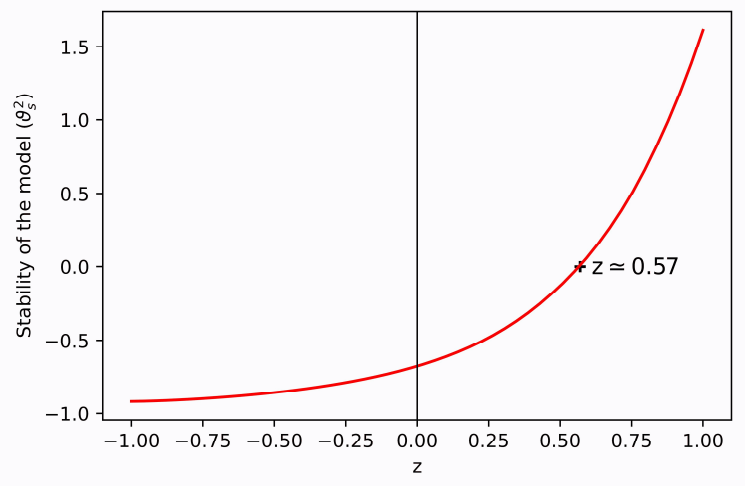

Figure 6: Shows the behavior of ϑ_s^2 versus z.

4.4. The anisotropic parameter (A_m)

The anisotropic parameter A_m of the universe plays a crucial role in understanding the anisotropic characteristics of the universe and deviations from isotropy. $A_m = 0$ indicates an

isotropic universe, while a constant value of A_m from early to late times implies that the universe remains anisotropic throughout its evolution.

Utilizing equations (31) through (34) in equation (15), the anisotropic parameter (A_m) of the universe is obtained as

$$A_m = -\frac{2\chi(z+1)^6}{3k^2\left[(z+1)^{\xi}+1\right]^2} \tag{43}$$

Figure 7 shows the behavior of the anisotropic parameter A_m of the universe with respect to redshift z. It is clear from the figure that A_m is a negatively increasing function of redshift z. It starts with a very small negative value at the initial phase of the universe and eventually reaches zero in the future, $i.e., A_m \to 0 \; as \; z \to -1$. This indicates that the universe currently exhibits anisotropic characteristics and will become isotropic in the future.

4.5. The torsion scalar $(\boldsymbol{T})$

The torsion scalar $\boldsymbol{T}$ is a fundamental quantity in the framework of teleparallel gravity provides a way to describe gravitational phenomena by focusing on the twisting of spacetime, offering a complementary perspective to the traditional curvature-based approach. It is constructed from the torsion tensor, effectively quantifies the overall twisting of spacetime that is, it measures how much and in what way spacetime is twisted. Larger magnitude values mean greater twisting, indicating a stronger deviation from a flat, untwisted spacetime.

Utilizing equations (31) through (34) in equation (16), the torsion scalar $(\boldsymbol{T})$ of the universe is obtained as

$$T = -6k^2\left[(z+1)^{\xi}+1\right]^2 - 2\chi(z+1)^6 \tag{44}$$

Figure 8 shows the behavior of torsion scalar (T) of the universe with respect to redshift z. It is clear from the figure that T is a negatively increasing function of redshift z. It starts with a very small negative value (i.e. very large in magnitude) at the early phase of the universe and gradually converges towards a negative value close to zero as $z \to -1$ in the future. This indicates that in the early phase of the universe, torsion is very high, and as time progresses, its influence gradually diminishes.

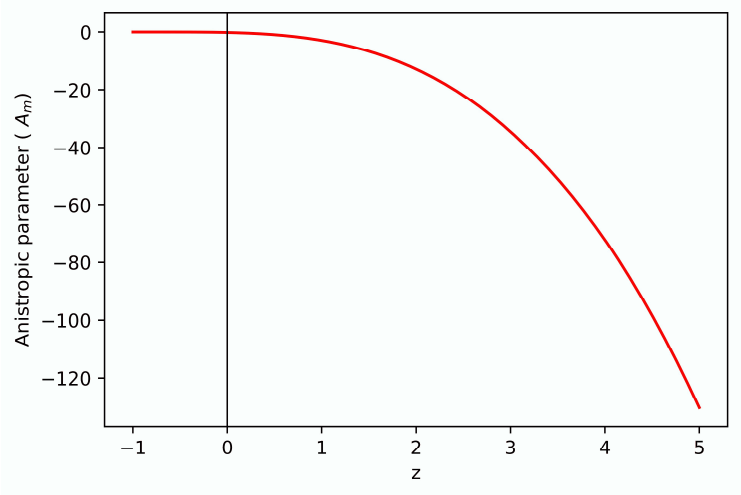

Figure 7: Shows the behavior of A_m versus z.

Figure 8: Shows the behavior of T versus z.

4.6. The energy conditions

The energy conditions derived from Raychaudhuri's equation [63] offer linear relationships between energy density and pressure, serving as vital tools for validating dark energy models and verifying the universe's accelerated expansion. This study focuses on three significant energy conditions: the null energy condition (NEC), the dominant energy condition (DEC), and the strong energy condition (SEC). By examining these conditions, we derive constraints that deepen our understanding of the model's dynamics and characteristics. These conditions are defined as follows [64]:

- Null energy condition (NEC): $\rho + p \geq 0$,
- Dominant energy condition (DEC): $\rho - p \geq 0$,
- Strong energy condition (SEC): $\rho + 3p \geq 0$,

Using equations (39) and (40), The energy conditions for our model can be expressed as

$$\rho(z)+p(z)=\alpha\left[\xi_1\left\{6k^2\left[(z+1)^{\xi}+1\right]^2+2\chi(z+1)^6\right\}+\xi_2\right]^2 \tag{45}$$

$$\rho(z)-p(z)=\left[\xi_1\left\{6k^2\left[(z+1)^{\xi}+1\right]^2+2\chi(z+1)^6\right\}+\xi_2\right]\left[2-\alpha\left\{\xi_1\left(6k^2\left[(z+1)^{\xi}+1\right]^2+2\chi(z+1)^6\right)+\xi_2\right\}\right] \tag{46}$$

$$\rho(z)+3p(z)=\left[\xi_1\{6k^2\left[(z+1)^{\xi}+1\right]^2+2\chi(z+1)^6\}+\xi_2\right]\left[3\alpha\left\{\xi_1(6k^2\left[(z+1)^{\xi}+1\right]^2+2\chi(z+1)^6)+\xi_2\right\}-2\right] \tag{47}$$

Figure 9 depicts the evolutionary behavior of the energy conditions with respect to redshift z. The Null Energy Condition (NEC) shows a positive decrease and approaches zero as time progresses

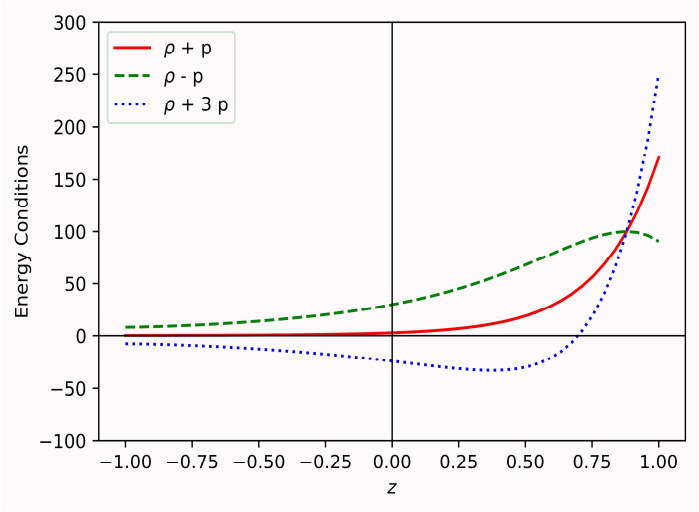

Figure 9: Shows the behavior of energy conditions versus z.

into the future. Similarly, the Dominant Energy Condition (DEC) also decreases positively but remains above zero. In contrast, the Strong Energy Condition (SEC) starts from a large positive value in the early universe and decreases, eventually turning negative in the present and future. This behavior indicates that both the NEC and DEC are satisfied throughout the evolution, whereas the SEC is violated in the present and future epochs. The violation of the SEC is significant as it implies the presence of a repulsive gravitational effect, leading to the accelerated expansion of the universe.

4.7. Deceleration parameter (q)

The deceleration parameter (q) is a cosmological quantity that describes whether the expansion of the universe is accelerating or decelerating. The dynamics and evolution of the universe can also be understood through the study of the deceleration parameter. The deceleration parameter

(q) can be expressed in terms of the Hubble parameter (H) as a function of redshift (z) as [65] follows:

$$q(z) = -1 + \frac{(z+1)}{H(z)}\frac{dH(z)}{dz} \tag{48}$$

Using equation (35) in equation (48), the deceleration parameter of the universe for our model as

$$q(z) = -1 + \frac{\xi(z+1)^{\xi}}{(z+1)^{\xi}+1} \tag{49}$$

The behavior of expansion of the universe is determined by the value of the deceleration parameter. $q > 0$ indicates that the expansion is decelerating, while $q < 0$ implies that the expansion is accelerating. Figure 10 shows the behavior of deceleration parameter with respect to redshift z. It can be observed from the figure that z as approaches -1, q approaches -1, indicating an accelerated expansion in the late-time universe. Additionally, the figure clearly demonstrates the transition of the universe from a decelerating phase to an accelerating phase. The current value of the deceleration parameter in our obtained model is $q_0 \approx -0.225$, with a transition redshift value of $z_t \approx 0.61$. In comparison, the standard ΛCDM model has a deceleration parameter of $q_0 \approx -0.56$ and a transition redshift of $z_t \approx 0.66$ [66]. Although there are differences between these values, they are relatively close. This suggests that our model's estimated values align reasonably well with those of the ΛCDM model, supporting the validity and reliability of our result.

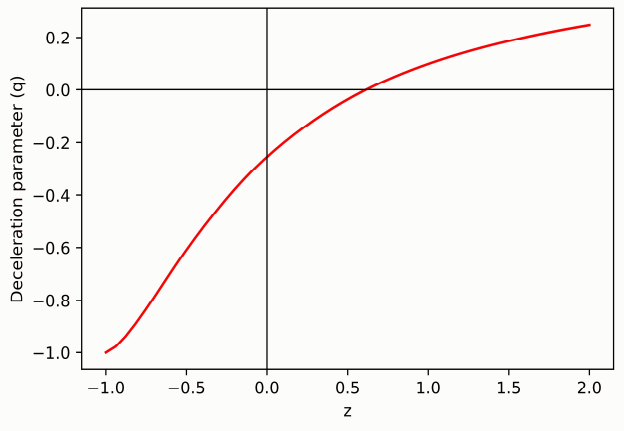

Figure 10: Shows the behavior of q versus z.

Therefore, we can conclude that the universe in our model was decelerating in the past and is currently accelerating, a trend expected to continue into the future.

4.8. Diagnostic parameters

In cosmology, the diagnostic parameters such as Statefinder diagnostic parameter and O_m diagnostic parameter plays an important role in understanding the history, evolution, and dynamics of the universe, as well as in distinguishing between different dark energy models.

4.8.1. Statefinder diagnostic parameter

An unknown form of energy behind the accelerating expansion of the universe is known as dark energy. Its precise nature remains unknown, making it a focal point of cosmological research. Several dark energy models have been proposed to understand the nature of dark energy. These models exhibit different behaviors when compared to each other. Sahni et al. [67] proposed a geometrical diagnostic tool to distinguish between different dark energy models, called the Statefinder diagnostic pair $\{r, s\}$. The r and s parameters in terms of redshift z are defined as follows:

$$r(z) = 1 - 2(z+1)\frac{H'(z)}{H(z)} + (z+1)^2\frac{H''(z)}{H(z)} + (z+1)^2\frac{[H'(z)]^2}{[H(z)]^2} \tag{50}$$

$$s(z) = \frac{r(z)-1}{3\left(q(z)-\frac{1}{2}\right)} \tag{51}$$

where $q(z) \neq \frac{1}{2}$. Moreover, The Statefinder diagnostic is a dimensionless quantity, meaning the values of the Statefinder parameters r and s are pure numbers without any physical units of measurement. This makes it useful for comparing different dark energy models and understanding the behavior of the universe's expansion without being influenced by specific units of measurement. The different combinations of r and s represent different dark energy models such as

- $\{r = 1, s = 0\}$ represents ΛCDM
- $\{r = 1, s = 1\}$ represents standard cold dark matter (SCDM)
- $\left\{r = 1, s = \frac{2}{3}\right\}$ represents holographic dark Energy (HDE)
- $\{r > 1, s < 0\}$ represents Chaplygin gas (CG)
- $\{r < 1, s > 0\}$ represents quintessence

Utilizing equations (35) and (49) in equations (50) and (51), the expression of r and s parameters for our obtained model as

$$r(z) = 1 + \frac{\xi(2\xi-3)(z+1)^{2\xi} + \xi(\xi-3)(z+1)^{\xi}}{\left[(z+1)^{\xi}+1\right]^2} \tag{52}$$

$$s(z) = \frac{2\xi(z+1)^{\xi}}{3\left[(z+1)^{\xi}+1\right]}\left(1 + \frac{\xi}{(2\xi-3)(z+1)^{\xi}-3}\right) \tag{53}$$

Figure 11 and 12 illustrate the behavior of the parameters r and s as a function of redshift z . As z approaches -1, we observe that r tends towards 1 and s approaches 0. Figure 13 further highlights the relationship between s and r. The star marked on the curve in Figure 13 represents the current values of the Statefinder parameters $(s_0 \simeq 0.1435, r_0 \simeq 0.4301)$. As z approaches -1, the parameters (s, r) converge to $(0,1)$. This analysis suggests that, in our model, the universe currently behaves like a quintessence dark energy model and tends towards the ΛCDM model at late times, indicating a spatially flat universe.

Moreover, In $r-q$ plane,

- $(r,q)=(1,0.5)$ which corresponds to SCDM which is a matter-dominated universe
- $(r,q)=(1,-0.56)$ aligns with ΛCDM
- $(r,q)=(1,-1)$ represents the de Sitter expansion (dS).

In Figure 14, we observe that as $z\to-1$ then $(r,q)\to(1,-1)$ indicating that at late times, expansion of the universe will be accelerating at a constant rate.

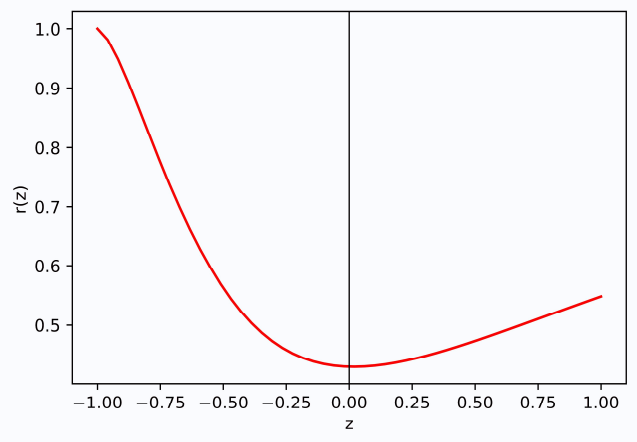

Figure 11: Shows the behavior of r versus z.

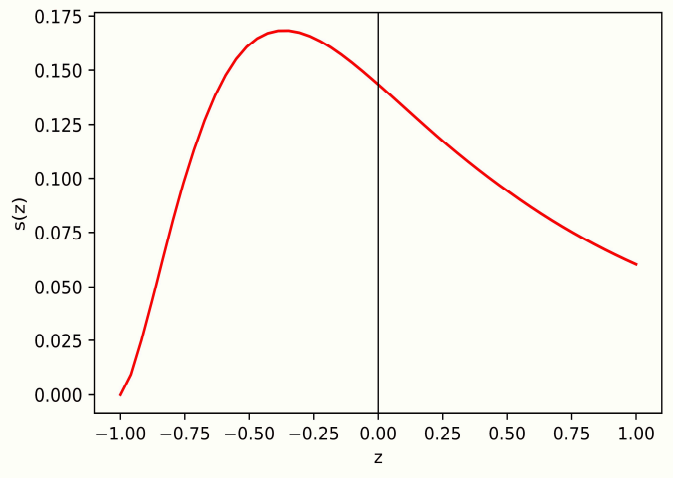

Figure 12: Shows the behavior of s versus z.

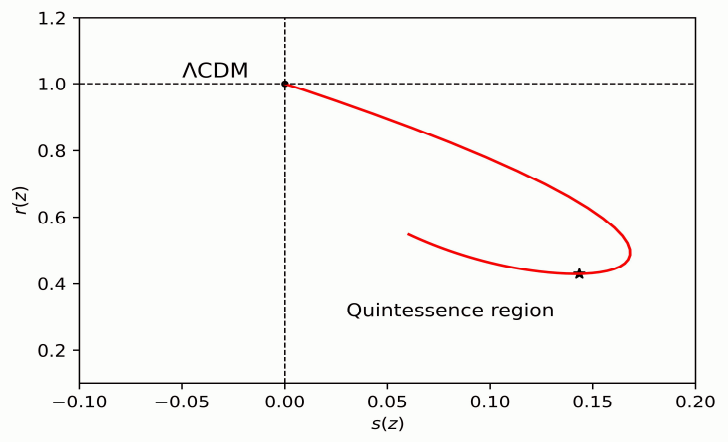

Figure 13: Shows the behavior of r versus s with star representing the current value.

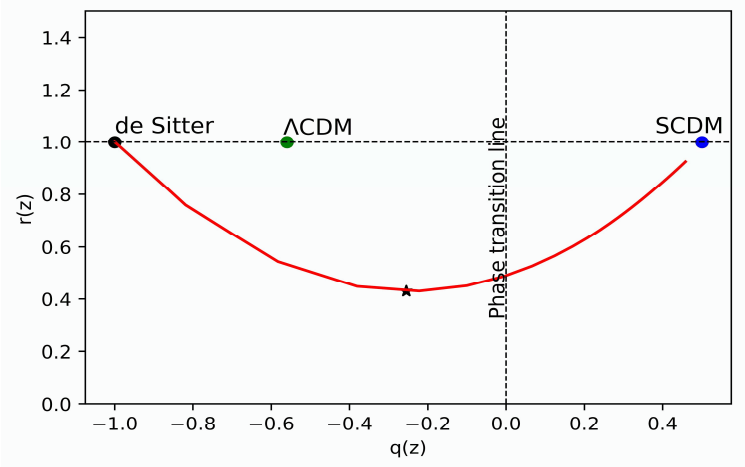

Figure 14: Shows the behavior of r versus q with star representing the current value.

4.8.2. O_m diagnostic parameter

To understand the dynamical nature of dark energy invaluable geometrical diagnostic tool was introduced by [68], which is constructed from the combination of Hubble parameter H and cosmological redshift z, which we know as Om(z) diagnostic. The $O_m(z)$ diagnostic in a standard form can be defined as

$$O_m(z) = \frac{\mathcal{F}^2(z)-1}{(z+1)^3-1} \tag{54}$$

where $\mathcal{F}(z) = \frac{H(z)}{H_0}$ and H_0 be the current Hubble constant. The $O_m(z)$ diagnostic for our obtained model is as follows

$$O_m(z) = \frac{[(z+1)^{\xi}+3]\,[(z+1)^{\xi}-1]}{4z(z^2+3z+3)} \tag{55}$$

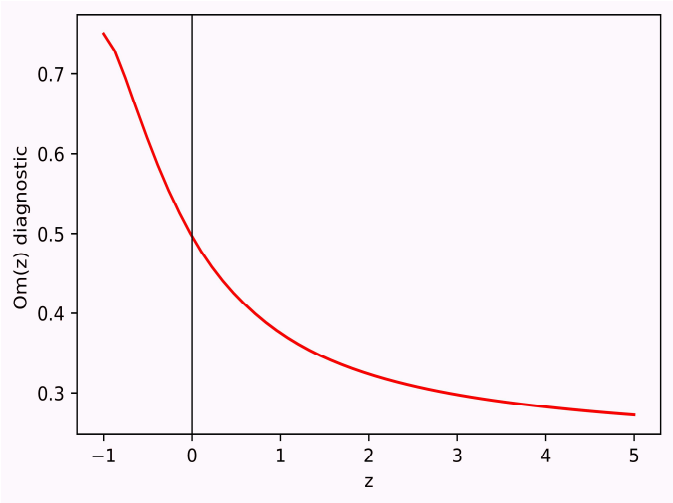

Figure 15: Shows the behavior of $O_m(z)$ diagnostic versus z.

The $O_m(z)$ diagnostic tool is utilized to determine the nature of dark energy models by examining its slope. A positive slope indicates a phantom nature with an equation of state value less than -1 $(i.e., \omega < -1)$, while a negative slope suggests a quintessence nature with an equation of state value greater than -1 $(i.e., \omega > -1)$. If the slope remains constant with respect to redshift, it implies the dark energy model aligns with the cosmological constant (ΛCDM). Figure 15 illustrates the evolution of $O_m(z)$ in our model. Observing Figure 15, we can see that the slope of $O_m(z)$ is negative, indicating that our model exhibits a quintessence nature.

5. Summary & Conclusion

This paper focuses on the investigation of the homogeneous and anisotropic Bianchi type-I spacetime within the framework of $f(T)$ gravity theory, utilizing a quadratic equation of state and a specific deceleration parameter. we presented the foundational mathematical framework of $f(T)$ theory of gravity following the introductory section of the article. Thereafter, we compared our cosmological model with Cosmic Chronometers (CC) dataset to determine key parameters such as ξ and H_0, using Bayesian statistical methods and the Markov Chain Monte Carlo (MCMC) technique to refine our analysis. Our analysis yields $\xi = 1.49^{+0.10}_{-0.10}$ and $H_0 = 65.04^{+2.47}_{-2.39}$.

Moreover, in our study, we selected the values of the free parameters as $\xi_1 = 0.55$, $\xi_2 = 0.45$, $k = 1.05$, $\chi = 1.1$ and $\alpha = 0.01$. we have determined the cosmological parameters as functions of redshift z and graphically depicted them to enhance our understanding of the universe's expansion and evolutionary history. The energy density ρ and pressure p decrease as z

approaches −1. However, the energy density remains positive throughout cosmic evolution, while the pressure becomes negative both in the present and in the future. This indicates that the universe is expanding and accelerating. The stability parameter indicates that the universe transitioned from stability to instability at redshift $z \simeq 0.57$ and will remain unstable in the future. The universe currently exhibits anisotropic characteristics but will become isotropic in the future as indicated by the anisotropic parameter A_m approaching 0 as z approaches -1 $(i.e., A_m \to 0 \; as \; z \to -1)$.

The graphical behavior of the torsion scalar T with respect to redshift z , as shown in Figure 6, indicates that torsion is very high in the early phase of the universe. As time progresses, its influence gradually diminishes. Moreover, in our study, we analyze the energy conditions, including the Null Energy Condition (NEC), Dominant Energy Condition (DEC), and Strong Energy Condition (SEC). Our findings reveal that both NEC and DEC are satisfied throughout the cosmic evolution. However, the SEC is violated in the present and future epochs. This violation of the SEC is significant as it implies the presence of a repulsive gravitational effect, leading to the accelerated expansion of the universe.

Additionally, the deceleration parameter demonstrates the transition of the universe from a decelerating phase to an accelerating phase. The current value of the deceleration parameter in our obtained model is $q_0 \approx -0.225$, with a transition redshift value of $z_t \approx 0.61$. Furthermore, The Statefinder diagnostic pair analysis favors the quintessence dark energy model in the present and tends towards the ΛCDM model at late times, whereas the $r - q$ plane analysis places our model in the quintessence region currently and indicates it will reach the de Sitter point in the future. The $O_m(z)$ diagnostic further indicates that our model exhibits a quintessence nature. In conclusion, our obtained model demonstrates that the universe is currently in an accelerated expansion phase, exhibits anisotropic characteristics, and will transition to an isotropic state in the future, while presently behaving like a quintessence dark energy model.

Appendix

31 points of $H(z)$ datasets by DA method					
z	$H(z)$	σ_H	z	$H(z)$	σ_H
0.070	69	19.6	0.4783	80.9	9.0
0.090	69	12	0.480	97	62
0.120	68.6	26.2	0.593	104	13.0
0.170	83	8	0.6797	92	8
0.1791	75	4	0.7812	105	12
0.1993	75	5	0.8754	125	17
0.200	72.9	29.6	0.880	90	40
0.270	77	14	0.900	117	23
0.280	88.8	36.6	1.037	154	20
0.3519	83	14	1.300	168	17

0.3802	83	13.5	1.363	160	33.6
0.400	95	17	1.430	177	18
0.4004	77	10.2	1.530	140	14
0.4247	87.1	11.2	1.750	202	40
0.4497	92.8	12.9	1.965	186.5	50.4
0.470	89	34			

Table1: The 31 Hubble parameter $H(z)$ data points and their errors σ_H from the CC data.

Acknowledgements:

Credit authorship contribution statement: **Syed Mudassir Syed Iqbal:** original draft, Investigation, Conceptualization, Graphs plotting, data curation, review and editing; **G. U. Khapekar:** Validation and Supervision. Both the authors have read and agreed to the published version of the manuscript.

Declaration of competing interest: The authors declare that they have no known competing financial interests or personal relationships that could have appeared to influence the work reported in this paper.

Data availability: There are no new data associated with this article.

Received October 13, 2024; Accepted December 29, 2024

References

[1] A. G. Riess et.al., *Astronomical J. 116*(3), 1009, (1998).

[2] S. Perlmutter et.al., *Astrophysical J*, *517*(2), 565, (1999).

[3] D.N. Spergel et.al., *Astrophysical J. Suppl. Ser. 148*(1), 175, (2003).

[4] D.N. Spergel et.al., *Astrophysical J. suppl. ser*, *170*(2), 377, (2007).

[5] M. Tegmark et.al., *Physical review D*, *69*(10), 103501, (2004).

[6] D. J. Eisenstein et.al., *Astrophysical J*, *633*(2), 560, (2005).

[7] S.M. Carroll, *Living reviews in relativity*, *4*(1), 1-56, (2001).

[8] E. J. Copeland et.al, *Inter. J. Mod. Phys. D*, *15*(11), 1753-1935, (2006).

[9] R.J. Yang et.al., *Mon. Not. Roy. Astro. Soc*, *407*(3), 1835-1841, (2010).

[10] T. P. Sotiriou et.al., *Rev. Mod. Phys*, *82*(1), 451, (2010).

[11] S. I. Nojiri et.al., *Phys. Lett. B*, *631*(1-2), 1-6, (2005).

[12] T. Harko et.al., *Phys. Rev. D*, *84*(2), 024020,(2011).

[13] G. R. Bengochea et.al., *Phys. Rev. D*, *79*(12), 124019, (2009).

[14] G. R. Bengochea et.at., *Phys. Let. B*, *695*(5), 405-411, (2011).

[15] Y. F. Cai et.al., *Reports Prog. Phys*, *79*(10), 106901, (2016).

[16] De Andrade et.al., *Gravitation and Relativistic Field Theories, 3,* 1022-1023, (2002).

[17] R. Aldrovandi et.al., Springer Science & Business Media,173, (2012).

[18] A. Einstein, *Mathematische Annalen*, *102*(1), 685-697, (1930).

[19] Unzicker, Alexander et.al., *arXiv preprint physics/0503046* (2005).

[20] R. Myrzakulov, *Euro. Phys. J. C*, *71*(9), 1752, (2011).

[21] S. Mandal, Sanjay, et al., *Physics of the Dark Universe* 28, 100551, (2020).

[22] S. H. Shekh et.al., *Astrophys. Space Sci.*, *365*(3), 60, (2020).

[23] V. J. Dagwal et.al., *Indian Journal of Physics*, *95*(9), 1923-1931, (2021).

[24] M. Koussour et.al., *Classical and Quantum Gravity*, *39*(10), 105001, (2022).

[25] D. D. Pawar et.al., *East European Journal of Physics*, (1), 102-111, (2024).

[26] V. J. *Indian Journal of Physics*, *98*(3), 1163-1177, (2024).

[27] L. K. Duchaniya, *Physics of the Dark Universe*, *44*, 101461, (2024).

[28] R. Briffa et.al., R., *Mont. Not. Roy. Astro. Soc.*, *528*(2), 2711-2727, (2024).

[29] N. Dimakis et.al., *Physical Review D*, *109*(2), 024031, (2024).

[30] P. H. Chavanis, *Universe*, *1*(3), 357-411, (2015).

[31] D. R. K. Reddy et.al., *Astrophys. Space Sci.*, *357*, 1-5, (2015).

[32] S. Capozziello et.al., *Physical Review D, 73*(4), 043512, (2006).

[33] J. Berteaud et.al., *J. Cosmo. Astropart. Phys.*, *2019*(10), 069, (2019).

[34] G. P. Singh et.al., *Advances in High Energy Physics*, *2015*(1), 816826, (2015).

[35] P. H. Chavanis, *Universe*, *1*(3), 357-411, (2015).

[36] S. R. Bhoyar et.al., *Prespacetime J.*, *7*(3), (2016).

[37] V. A. Thakare et.al., *East Eur. J. Phys.*, (3), 108-121, (2023).

[38] C. R. Mahanta et.al., *East Eur. J. Phys.*, (1), 44-52, (2023).

[39] M. E. Rodrigues et.al., *Phys. Rev. D*, *86*(10), 104059, (2012).

[40] F. B. M. dos Santos, *J. Cosmo. Astropart. Phys.*, *2023*(06), 039, (2023).

[41] A. Linde, Springer, Berlin, Heidelberg, 1-54, (2008).

[42] Ade, Peter AR, et al., Astronomy & Astrophysics 571, A12, (2014).

[43] K. Saaidi et.al., *Astrophys. Space Sci.*, *341*, 657-662, (2012).

[44] H. Hossienkhani et.al., *Phys. dark univ.*, *18*, 17-29, (2017).

[45] M. Koussour et.al., *Afrika Matematika*, *33*(1), 27, (2022).

[46] S. Singhal et.al., *Bulg. J. Phys.*, *50*(2), (2023).

[47] A. Banerjee et.al., *J. math. phys.*, *26*(11), 3010-3015, (1985).

[48] A. Banerjee et.al., *Pramana*, *34*, 1-11, (1990).

[49] K. D. Krori et.al., *Gen. Rela. Gravit.*, *26*, 265-274, (1994).

[50] S. S. Xulu, *Inter. J. Theo. Phys.*, *39*, 1153-1161, (2000).

[51] O. AydoĞdu et.al., *Astrophys. Space Sci.*, *299*, 227-232, (2005).

[52] L. L. So et.al., *arXiv preprint gr-qc/0611012*, (2006).

[53] A. K. Singha et.al., *Inter. J. Theo. Phys.*, *48*, 351-356, (2009).

[54] D. W. Hogg et.al., *Astrophys. J. Supple. Seri.*, *236*(1), 11, (2018).

[55] R. Jimenez., *Astrophys. J.*, *573*(1), 37, (2002).

[56] P. Mukherjee et.al., *Euro. Phys. J. C*, *81*(1), 36, (2021).

[57] P. Bessa et.al., *European Physical Journal C*, *82*(6), 506, (2022).

[58] P. Mukherjee, *arXiv preprint arXiv:2207.07857*, (2022).

[59] D. Mhamdi et.al., *Euro. Phys. J. C*, *84*(3), 310, (2024).

[60] G. B. Zhao et.al., *Phys. Rev. D*, *72*(12), 123515, (2015).

[61] J. Q. Xia et.al., *Inter. J. Mod. Phys. D*, *17*(08), 1229-1243, (2008).

[62] M. Koussour et.al., *Nuclear Phys. B*, *990*, 116158, (2023).

[63] A. Raychaudhuri, Relativistic cosmology. I. *Physical Review*, *98*(4), 1123, (1955).

[64] S. Mandal et.al., *Phys. Rev. D*, *102*(2), 024057, (2020).

[65] Y. Xu et.al., *Euro. Phys. J. C*, *79*, 1-19, (2019).

[66] N. Aghanim et.al., *Astronomy & Astrophysics*, *641*, A6, (2020).

[67] V. Sahni et.al., *J. Experi. Theo. Phys. Lett.*, *77*, 201-206, (2003).

[68] V. Sahni et.al., *Phys. Rev. D, 78*(10), 103502, (2008).